

On Merits of Faster-than-Nyquist Signaling in the Finite Blocklength Regime

Yong Jin Daniel Kim, *Member, IEEE*

Abstract—We identify potential merits of faster-than-Nyquist (FTN) signaling in the finite blocklength (FBL) regime. A unique aspect of FTN signaling is that it can increase the blocklength by packing more data symbols within the same time and frequency to yield strictly higher number of independent signaling dimensions than that of Nyquist rate signaling. Using the finite-blocklength information theory, we provide tight bounds on the maximum channel coding rate (MCCR) of FTN signaling for any finite time-bandwidth product. The merits are categorized into two operating regions of FTN, i.e., when the time-acceleration factor of FTN, τ , is above or below a certain threshold τ_0 . When $\tau > \tau_0$, FTN has both higher channel capacity and MCCR than that of Nyquist rate signaling, when the utilized pulse shape is non-sinc. Since the issues associated with the ideal sinc pulse only get exacerbated when packets are short, the benefit of FTN becomes more significant in the FBL regime. On the other hand, when $\tau < \tau_0$, the channel capacity is fixed but MCCR of FTN can continue to increase to a certain degree, thereby reducing the gap between the capacity and MCCR. This benefit is present regardless of the utilized pulse shape, including the ideal sinc-pulse, and is unique to the FBL regime. Instead of increasing MCCR for fixed block error rates, FTN can alternatively lower the block error rates for fixed channel coding rates. These results imply that FTN can lower the penalty from limited channel coding over short blocklength and can improve the performance and reliability of short packet communications.

Index Terms—Channel capacity, faster-than-Nyquist signaling, finite blocklength regime, channel coding rate.

I. INTRODUCTION

The Nyquist sampling theorem asserts that strictly bandlimited sinc pulses, that are transmitted at the Nyquist rate of $2W$ pulses per second over a bandlimited channel, are orthogonal and may represent any signals of bandwidth W Hz. In practice, sinc pulses cannot be used due to being non-causal, having long tails that decay slowly as $1/t$ in time t , and being highly sensitive to any synchronization mismatch. Practical pulse-shaping (such as the root-raised cosine (RRC) pulses), however, introduces excess bandwidth, resulting in lower signaling rates to maintain orthogonality and incurring penalties in the performance.

The faster-than-Nyquist (FTN) signaling has been successfully applied to regain the loss due to the practical pulse-shaping [1], [2], [3]. In the FTN literature, the Nyquist rate is generally defined as the maximal signaling rate to guarantee orthogonality between the pulses. By deliberately

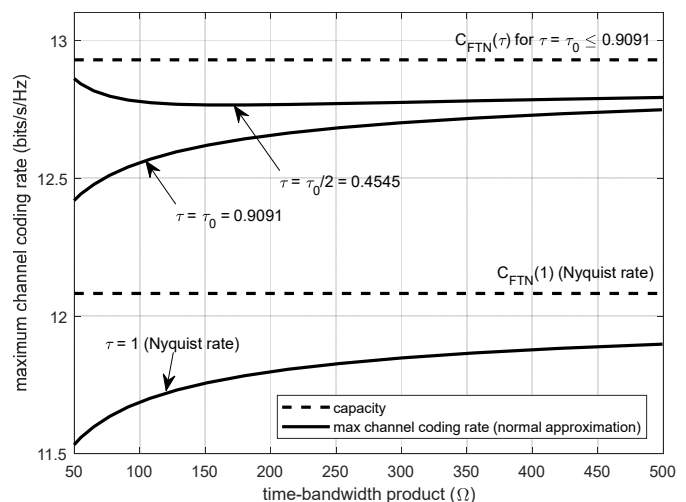


Fig. 1. Plotting the channel capacity and the maximum channel coding rates (the normal approximation) of FTN signaling in the FBL regime. Assuming RRC pulse with roll-off factor 0.1 at 40 dB SNR and 10^{-3} block error rate and varying FTN time-acceleration factor τ .

signaling above the Nyquist rate, it has been demonstrated that FTN signaling can minimize the loss from using practical pulse-shaping and achieve the generalized Shannon capacity of bandlimited channel for any arbitrary pulse-shape [4]. The capacity gain comes at the expense of generating an inter-symbol interference (ISI), but the structure of ISI is deterministic in an FTN system and may be compensated by precoding and/or equalization techniques. Exponential growth in the available computing power and the recent advancements in the equalization and coding theory have allowed practical coding designs for FTN that can perform close to its theoretical capacity limit (see e.g., [5]-[9]).

Recently there has been a rising interest in designing (and optimizing) systems operating in a finite blocklength (FBL) regime, i.e., in the order of a few hundreds of coded bits, due to the advent of delay sensitive applications that also demand high reliability – such as Tactile Internet, factory automation, and virtual/augmented reality [10]. For example, one of the three key features of the 5G has been the ultra-reliable low latency communication (URLLC), which is expected to provide a guaranteed quality of service to mission-critical communications that are under stringent latency and high reliability requirements [11].

A number of interesting problems arise when communicating in the FBL regime. First, the block error rates (BLER) can no longer vanish for most channels of interest, and for a nonzero target BLER, there usually exists a penalty in the maximum achievable rates compared to the channel capacity. This implies

that there exist intricate tradeoffs between data rates (performance), block error rates (reliability), and blocklength (latency). Second, ideal pulse shapes such as the sinc pulse or the RRC pulse with very small roll-off factor entail higher costs from having long tails in the time domain. Arguments such as the cost of the excess tails of the pulse shapes being amortized over a long blocklength are more difficult to justify in the FBL regime. Third, Nyquist rate signaling with the ideal sinc pulse is no longer theoretically optimal in the FBL regime. This is because the Nyquist sampling theorem, which Nyquist rate signaling is based on, assumes that the samples are taken over a long period of time. If the sampling window is restricted to a finite time interval, it is necessary to sample faster than the Nyquist rate to accurately represent any bandlimited signals (accuracy here is in terms of L_2 error [12]).

In this work, we investigate FTN signaling to overcome some of these problems present in the FBL regime. One unique aspect of FTN signaling is that the blocklength N can be increased indefinitely for a fixed time and frequency, by packing more data symbols in the same time span and bandwidth. Using the finite-blocklength information theory, we provide accurate bounds on the maximum channel coding rates (or alternatively, the minimum BLER) of FTN signaling for any time-bandwidth product. Several potential merits to using FTN signaling in the FBL regime are then identified.

The merits are categorized under two disjoint operating regions of FTN signaling: 1) when the time-acceleration factor of FTN, $\tau < 1$, is above a certain threshold τ_0 (which is equal to $(1+\beta)^{-1}$ when the RRC pulse with roll-off factor β is being used), and 2) when τ is below τ_0 . Note that $\tau = 1$ yields Nyquist rate signaling and decreasing τ results in speeding up the signaling rate of FTN. In the first region of $\tau \geq \tau_0$, both the channel capacity and the maximal channel coding rates (MCCR) can increase as τ approaches the threshold τ_0 . This implies that the rate benefit of FTN is also present in the FBL regime. In the second region of $\tau < \tau_0$, on the other hand, the capacity of FTN remains fixed but MCCR of FTN can further increase and reduce the gap between the capacity and MCCR.

These benefits may be observed in Fig. 1, where normal approximations of MCCR are plotted for $\tau = 1$ (Nyquist rate), $\tau = \tau_0$, and $\tau = \tau_0/2$. The RRC with $\beta = 0.1$ is considered, for which $\tau_0 = 0.9091$. It is observed that the capacity (in dashed lines) increases as τ decreases until τ_0 . Meanwhile, MCCR (in solid lines) also increases to match the increasing capacity. For $\tau < \tau_0$, the capacity is fixed but MCCR is further increased, thereby reducing the penalty in the achievable rates in the FBL regime.

The main goal of this work is to accurately characterize MCCR and the minimum BLER of FTN and identify potential merits to signaling faster than the Nyquist rate in the FBL regime. The contributions of this work are summarized below:

- A normal approximation of MCCR of complex-valued *i.i.d.* FTN signaling is derived for any signaling rates. This extends the normal approximation derived for real-valued FTN signaling with $\tau = \tau_0$ in [13] to complex-valued FTN with arbitrary $\tau < 1$.
- An upper-bound and a lower-bound of MCCR are derived for FTN signaling. We use the meta-converse bound [14] for the upper-bound and the random-coding union (RCU) achievability bound [14] for the lower-bound. Numerical

results reveal that these bounds are tight for most scenarios of interests and the normal approximation falls between these bounds in most scenarios of interests.

- An asymptotic expansion of the meta-converse bound is provided to show that the derived normal approximation is accurate up to the order of Ω^{-1} , where Ω is the time-bandwidth product (TBP).
- The merits of FTN signaling are categorized for $\tau_0 \leq \tau < 1$ and $\tau < \tau_0$ in the FBL regime. For $\tau_0 \leq \tau < 1$, both the channel capacity and MCCR are shown to increase as τ decreases while the gap between them remains relatively constant. Similarly, for fixed channel coding rates, BLER can decrease as τ decreases.
- For $\tau < \tau_0$, it is shown that the gap between the capacity and MCCR can be reduced as τ decreases. The degree to which the gap is reduced depends on various factors including τ , SNR, and blocklength. The benefit is higher for smaller blocklength and higher channel SNR, and is present regardless of the pulse shapes. Similarly, for a fixed channel coding rate, BLER can be further reduced by signaling $\tau < \tau_0$. The benefit is higher for smaller blocklength and higher coding rates.
- We also study MCCR when FTN signaling employs finite constellation symbols. It is shown through numerical simulations that, for a fixed TBP and when the modulation symbols are binary, the effective FTN channel input approaches Gaussian with sufficiently small τ . This implies that accelerating the signaling rate (while TBP is held constant) has the same effect as increasing the modulation order, and the presented channel coding rates can be achieved while using finite constellation symbols with sufficiently small τ .

This paper is organized as follows. Section I.A provides a simple explanation of the threshold τ_0 and relates it to independent signaling dimensions available to an FTN system. Section II presents a discrete-time parallel Gaussian channel model for the considered FTN signaling. Section III develops the channel capacity, normal approximation, and upper- and lower-bounds of MCCR of FTN signaling. Asymptotic expansion of the meta-converse bound is also provided in this section. Section IV provides numerical results and discussions on the merits of FTN signaling in the FBL regime. Summary and future research directions are given in Section V.

A. Simple Explanation of the Threshold τ_0

Let T_d be the time duration in seconds and W be the bandwidth in Hz allotted for communication. When T_d is large, there exist approximately $2WT_d$ independent signaling dimensions within the time interval $(-T_d/2, T_d/2)$ and in the frequency band $(-W, W)$. This is known as the *2WT theorem* [15], [16], which is a direct consequence of the Nyquist sampling theorem. Let T be the smallest symbol time of an orthogonal signaling. In an FTN system, data symbols are sent at an accelerated rate of $(\tau T)^{-1}$ symbols per seconds ($\tau < 1$). The total time duration needed to send a block of N symbols is about $T_d = N\tau T$ seconds. If the utilized modulating pulse is RRC with roll-off factor β , the bandwidth is $W = (1+\beta)/(2T)$.

Then, due to the *2WT* theorem, in an FTN system there exists

$$N^* \approx 2WT_d \approx 2W(N\tau T) = (1+\beta)N\tau$$

number of independent signaling dimensions for transmitting N data symbols. Let $\tau_0 \triangleq (2WT)^{-1} = (1+\beta)^{-1}$. If $\tau > \tau_0$, N is strictly less than N^* and hence we are not utilizing N^*-N number of signaling dimensions. It is worth noting that Nyquist rate signaling ($\tau = 1$) is always underutilizing the space unless $\tau_0 = 1$ (i.e., the sinc pulse is used).

In the case of T_d small (i.e., in the FBL regime), there exists strictly greater than $2WT_d$ independent signaling dimensions (more accurately, $2WT_d(1+\eta)$ for some nonzero η [15]). In sections II and III, through channel modeling and FBL analysis, it is demonstrated that signaling with τ strictly below τ_0 is required to utilize to the entire signaling dimensions available in the FBL regime, and FTN signaling provides a practical means to utilize these additional signaling dimensions.

B. Notations

Superscripts $(\cdot)^*$ denote complex conjugation and j denotes imaginary unit. $\delta[n]$ denotes Kronecker-delta function. Bold-faced letters such as \mathbf{x} and \mathbf{A} denote column vectors and matrices. \mathbf{x}^T and \mathbf{x}^\dagger denote transpose and Hermitian of \mathbf{x} , respectively, and $\text{tr}(\mathbf{A})$ denotes trace of a matrix \mathbf{A} .

II. DISCRETE-TIME FTN CHANNEL MODEL

A discrete-time channel model of FTN signaling is developed. Assumptions on the considered FTN system model, approximate SNR distribution of the FTN channels, and the definition of time-bandwidth product are also provided.

A. System Model and Assumptions

In the FTN system, data symbol is sent at every τT seconds, where $\tau < 1$ is referred to as the time-acceleration factor (or the symbol packing ratio) of FTN. The total time duration needed to send a block of N symbols is about $N\tau T$ seconds. (The exact time duration is $(N-1)\tau T$, plus length of the modulating pulse-shape which is independent of both τ and N .) The complex baseband model of a FTN signal $x(t)$ is given by

$$x(t) = \sqrt{P\tau T} \sum_{n=0}^{N-1} x_n s(t - n\tau T), \quad (1)$$

where $x_n \in \mathbb{C}$ denotes the n^{th} data symbol, P denotes the average power

$$P = \mathbb{E} \left[\frac{1}{N\tau T} \int_{-\infty}^{\infty} |x(t)|^2 dt \right], \quad (2)$$

and $s(t)$ is a real-valued modulating pulse with unit energy and assumed to satisfy the T -orthogonality condition, i.e., T is the smallest positive real value such that $\int_{-\infty}^{\infty} s(t)s(t-nT)dt = 0$ for all non-zero integer n . We let $\hat{s}(f)$ be the Fourier transform of $s(t)$ and assume it bandlimited to $(-W, W)$ Hz.

When the symbols $\{x_n\}$ are wide-sense stationary, i.e., they have constant mean and autocorrelation $R[m-n] \triangleq \mathbb{E}\{x_n x_m^*\}$ that depends only on the difference $m-n$, the power spectral density (PSD) of the FTN signal $x(t)$ may be written as [17]

$$\mathcal{S}_x(f) = P |\hat{s}(f)|^2 \sum_{k=-\infty}^{\infty} R[k] e^{jk2\pi f\tau T}. \quad (3)$$

Note that PSD becomes simply $P|\hat{s}(f)|^2$ and independent of the time-acceleration factor τ if $R[k] = \delta[k]$. In light of this observation, we restrict our attention to $\{x_n\}$ that are uncorrelated and identically distributed (*i.i.d.*) with zero mean and unit variance, i.e., $\mathbb{E}\{x_n x_m^*\} = \delta[m-n]$, to keep PSD fixed regardless of τ . It is worth noting that higher capacity (and higher MCCR in the FBL regime) may be obtained by precoding or allocating power non-uniformly across the symbols [18], [13], but these necessarily alter the shape of PSD and can result in bandwidth expansion if not designed carefully [17].

We consider FTN signaling over a complex AWGN channel with flat PSD N_0 , and a matched filter receiver that is sampling at the FTN signaling rate of $(\tau T)^{-1}$ samples per second. The matched filter outputs (normalized by $\sqrt{N_0}$) may be expressed in a matrix equation as

$$\mathbf{y} = \sqrt{\rho\tau} \cdot \mathbf{H}\mathbf{x} + \mathbf{z}, \quad (4)$$

where $\rho \triangleq PT/N_0$ is the signal-to-noise ratio (SNR)¹, and $\mathbf{y} = [y_0, y_1, \dots, y_{N-1}]^T$, $\mathbf{x} = [x_0, x_1, \dots, x_{N-1}]^T$, and $\mathbf{z} = [z_0, z_1, \dots, z_{N-1}]^T$ are $N \times 1$ column vectors of the matched filter outputs, the data symbols, and additive (colored) Gaussian noise samples, respectively. The FTN channel matrix, \mathbf{H} , is $N \times N$ Toeplitz

$$\mathbf{H} = \begin{bmatrix} h_0 & h_{-1} & \cdots & h_{-(N-1)} \\ h_1 & h_0 & \cdots & h_{-(N-2)} \\ \vdots & \vdots & \ddots & \vdots \\ h_{N-1} & h_{N-2} & \cdots & h_0 \end{bmatrix}, \quad (5)$$

where $\{h_n\}$ are the samples of the autocorrelation of $s(t)$, i.e.,

$$h_n = \int_{-\infty}^{\infty} s(t)s(t-n\tau T)dt \text{ for } n \in \mathbb{Z}. \quad (6)$$

The FTN channel matrix captures ISI inherent in FTN signaling. Note that \mathbf{H} is symmetric for real-valued modulating pulse. The additive Gaussian noise vector \mathbf{z} is colored with zero mean and covariance matrix equal to the FTN channel matrix, i.e., $\text{cov}(\mathbf{z}) = \mathbf{H}$. When the modulating pulse is RRC with roll-off factor β , $\{h_n\}$ are simply the time samples of the raised-cosine pulse, hence

$$h_n = \begin{cases} \frac{\text{sinc}(n\tau)\cos(\pi\beta n\tau)}{1-(2\beta n\tau)^2}, & n \neq \pm 1/(2\beta\tau) \\ (\beta/2)\sin(\pi/(2\beta)), & n = \pm 1/(2\beta\tau). \end{cases} \quad (7)$$

An important property of \mathbf{H} is that it is always full rank (thus non-singular) in the FBL regime.

Lemma 1 (full rank [19]): When N is finite and $s(t)$ is either strictly time-limited or strictly band-limited, \mathbf{H} is non-singular.

B. N-Parallel Complex Gaussian Channel Model for FTN

The FTN channel may be conveniently decomposed into a set of parallel Gaussian channels by applying the

¹ The SNR, $\rho = PT/N_0$, is defined so that it is independent of τ .

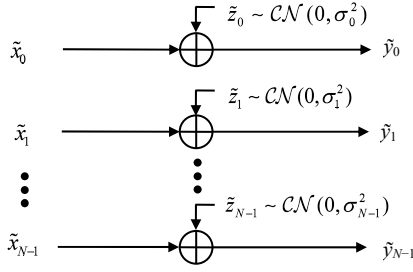


Fig. 2. N -parallel (complex) Gaussian channel formulation of FTN signaling where the variance of the noise in the n^{th} channel is $\sigma_n^2 = (\rho\tau\lambda_n)^{-1}$.

eigen-decomposition on the channel matrix, $\mathbf{H} = \mathbf{U}\mathbf{\Lambda}\mathbf{U}^T$, where \mathbf{U} is orthogonal whose columns are the eigenvectors of \mathbf{H} , and $\mathbf{\Lambda}$ is diagonal whose diagonal entries, $\{\lambda_n\}$, are the corresponding eigenvalues of \mathbf{H} . Letting $\tilde{\mathbf{x}} \triangleq \mathbf{U}^T \mathbf{x}$, $\mathbf{y}_u \triangleq \mathbf{U}^T \mathbf{y}$, and $\mathbf{z}_u \triangleq \mathbf{U}^T \mathbf{z}$ as orthogonal transformations, the FTN channel may be expressed as

$$\mathbf{y}_u = \sqrt{\rho\tau} \cdot \mathbf{\Lambda} \tilde{\mathbf{x}} + \mathbf{z}_u, \quad (8)$$

which yields a set of N parallel Gaussian channels with the effective channel gains $\{\sqrt{\rho\tau} \cdot \lambda_n\}$ and *uncorrelated* Gaussian noise vector \mathbf{z}_u with zero mean and diagonal covariance matrix equal to $\mathbf{\Lambda}$. Note that if \mathbf{x} is *u.i.d.*, $\tilde{\mathbf{x}}$ is also *u.i.d.* due to $\text{cov}(\mathbf{x}) = \text{cov}(\tilde{\mathbf{x}})$. If $\tilde{\mathbf{x}}$ can be decoded successfully, the original data symbols can be obtained by $\mathbf{x} = \mathbf{U}\tilde{\mathbf{x}}$.

It will be convenient to further normalize (8) by $\sqrt{\rho\tau} \cdot \mathbf{\Lambda}$ (possible due to the eigenvalues $\lambda_n > 0$ for all n due to Lemma 1). This leads to the following N -parallel complex Gaussian channel model of FTN:

$$\tilde{\mathbf{y}} = \tilde{\mathbf{x}} + \tilde{\mathbf{z}}, \quad (9)$$

where the input symbols $\{\tilde{x}_n\}$ are *u.i.d.* with zero mean and unit variance (i.e., $\text{cov}(\tilde{\mathbf{x}}) = \mathbf{I}$), and the *independent* Gaussian noise $\tilde{z}_n \sim \mathcal{CN}(0, \sigma_n^2)$ have variance $\sigma_n^2 \triangleq (\rho\tau\lambda_n)^{-1}$. Fig. 2 illustrates the FTN channel model (9). The SNR of n^{th} channel is given by $1/\sigma_n^2 = \rho\tau\lambda_n$.

Requiring $\text{cov}(\tilde{\mathbf{x}}) = \mathbf{I}$ means that the input must satisfy the *average* power constraint, $\mathbb{E}\{|\tilde{x}_n|^2\} = 1$ for all n . In the FBL analysis, sometimes it will be convenient to impose a stricter condition of constant input power for all realizations, i.e., $|\tilde{x}_n|^2 = 1$ for all n . The constant power implies that $\frac{1}{N}\|\mathbf{x}\|^2 = 1$ (i.e., equal power for individual codewords) due to $\|\mathbf{x}\| = \|\tilde{\mathbf{x}}\|$. We shall show that the inputs $\{\tilde{x}_n\}$ under the constant power constraint can achieve the channel capacity as the blocklength tends to infinity. The type of constraint used will be stated explicitly in the FBL analysis.

C. Eigenvalue distribution of the FTN Matrix

As evident from the parallel channel model formulation (9), the eigenvalues of the FTN matrix, $\{\lambda_n\}$, determine the quality

levels of the individual channels. While closed-form expression for these eigenvalues is unavailable for finite blocklength N , their properties, including asymptotic convergence (as $N \rightarrow \infty$ for fixed τ), are known and summarized in this section.

Due to Lemma 1, the eigenvalues $\{\lambda_n\}$ are strictly positive and add to N , i.e., $\sum_{n=0}^N \lambda_n = \text{tr}(\mathbf{H}) = N$, since the diagonal entries of \mathbf{H} , h_0 , are all equal to 1 for unit energy modulating pulses. Furthermore, the eigenvalues (disregarding its arbitrary order) asymptotically approach

$$\lambda_n \approx (\tau T)^{-1} \hat{s}_{\text{folded}}(f_n) \text{ for } f_n = n/(N\tau T), \quad (10)$$

where $\hat{s}_{\text{folded}}(f)$, called the *folded-spectrum*, is defined as

$$\hat{s}_{\text{folded}}(f) \triangleq \sum_{k=-\infty}^{\infty} |\hat{s}(f - k/(\tau T))|^2. \quad (11)$$

Proof involves the Szegő's theorem for asymptotic eigenvalue distribution of Toeplitz matrices [19]. In other words, the eigenvalues converge to sample values of the folded-spectrum. Closed-form expressions for the folded-spectrum are available for many modulating pulses of interest [19], and for RRC it is:

$$\hat{s}_{\text{folded}}(f) = |\hat{s}(f)|^2 + |\hat{s}(f - \frac{1}{\tau T})|^2, \quad (12)$$

for $f \in (0, (\tau T)^{-1})$ (and repeats every $(\tau T)^{-1}$ in f due to the periodicity of the folded-spectrum).

Fig. 3 plots the SNR distribution of the N -parallel Gaussian channel model of FTN, i.e., $1/\sigma_n^2 = \rho\tau\lambda_n$ sorted in the decreasing order, where the eigenvalues are either numerically computed from \mathbf{H} or approximated by (10). We assume the RRC pulses with $\beta = 0.5$, $\rho = 1$ (0 dB), and (τ, N) pairs chosen so that the total time interval T_d needed to transmit N FTN symbols is fixed. We can observe that the number of eigenchannels with nonzero SNRs grows with the increasing FTN signaling rates $(\tau T)^{-1}$.

We note that the accuracy of the approximation (10) depends on the blocklength N . While the approximation can be accurate for moderate or large N with fixed τ for many modulating pulses of interest, it may still be inadequate in the FBL regime with very small blocklength and small FTN time-acceleration factor τ . For this reason, all reported results in this work are based on numerical computations of the eigenvalues.

D. Time-Bandwidth Product Ω

FTN signaling operates in the continuous-time domain, compressing the overall time interval needed to send N data symbols by a factor of $\tau < 1$. As such, comparing the rates of FTN systems with different τ may be ambiguous if plotted in terms of blocklength N (which is a common practice in the FBL literature), because within a finite time interval T_d , FTN can pack unlimited number of symbols ($N \rightarrow \infty$) by taking $\tau \rightarrow 0$. To remove such ambiguities, we define the time-bandwidth product (TBP) as

$$\Omega \triangleq 2WT_d \approx 2WN\tau T \text{ [s}\cdot\text{Hz]}, \quad (13)$$

and formulate our problem as finding MCCRs for a *fixed* TBP Ω . This will allow us to study how the gap between the capacity and MCCR changes when more symbols are packed

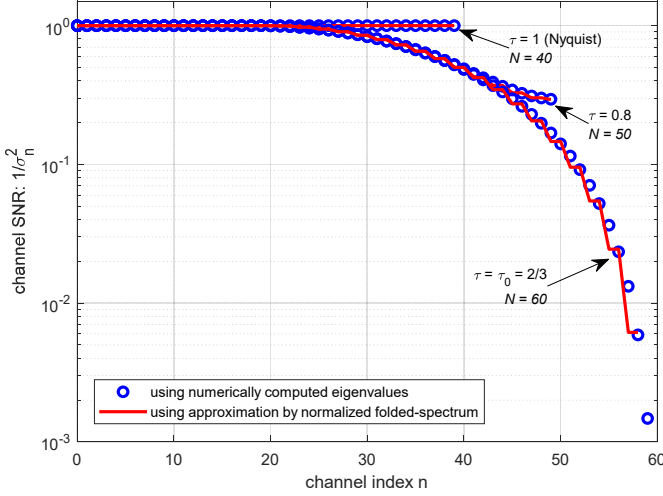


Fig. 3. SNR distribution of the N -parallel Gaussian channel model of FTN signaling, generated by either numerically computing the eigenvalues of the FTN channel matrix \mathbf{H} or approximating them by normalized folded-spectrum. (τ, N) pairs are chosen so that the time-bandwidth product is fixed at 60.

within a fixed TBP Ω . With this definition, the FTN symbol rate is N/Ω in symbols/s/Hz. With RRC pulses, TBP becomes $\Omega \approx N\tau(1 + \beta)$. It is also worth noting that TBP is equal to the maximum number of independent signaling dimensions in the asymptotic blocklength regime as discussed in Section I.A.

III. MAXIMUM CHANNEL CODING RATE OF FTN SIGNALING

This section presents the channel capacity and normal approximation and bounds on MCCR of FTN signaling.

A. Capacity of FTN Signaling

The channel capacity of FTN signaling (in the asymptotic blocklength regime) was first derived in [4]. Here, for completeness, we recover the same result using the N -parallel Gaussian channel model of FTN (9) by following the approach in [19]. The capacity of the N -parallel Gaussian channel with SNR in the n^{th} channel equal to $1/\sigma_n^2$ is given by [20]

$$C = \lim_{N \rightarrow \infty} \frac{1}{N\tau T} \sum_{n=0}^{N-1} \log_2 \left(1 + \frac{1}{\sigma_n^2} \right) \text{ [bps]}.$$

Using $\sigma_n^2 = 1/(\rho\tau\lambda_n)$ and the asymptotic distribution of the eigenvalues $\lambda_n \approx (\tau T)^{-1} \hat{s}_{\text{folded}}(f_n)$ for $f_n = n/(N\tau T)$ due to (10), we may form a Riemann sum that converges in the limit as

$$\begin{aligned} C &= \lim_{N \rightarrow \infty} \frac{1}{N\tau T} \sum_{n=0}^{N-1} \log_2 \left(1 + \frac{\rho \hat{s}_{\text{folded}}(f_n)}{T} \right) \\ &= \int_0^{1/(\tau T)} \log_2 \left(1 + \frac{\rho \hat{s}_{\text{folded}}(f)}{T} \right) df \text{ [bps]}. \end{aligned}$$

In terms of the spectral efficiency in bits per second per Hz (bps/Hz), the capacity of FTN signaling may be expressed as

$$C_{FTN}(\tau) = \frac{1}{2W} \int_0^{1/(\tau T)} \log_2 \left(1 + \frac{\rho \hat{s}_{\text{folded}}(f)}{T} \right) df \text{ [bps/Hz]} \quad (14)$$

It should be noted that the above expression holds for any τ . The capacity reaches maximum when $\tau = \tau_0$, and for all $\tau \leq \tau_0$, it becomes a fixed constant given by:

$$C_{FTN}(\tau_0) = \frac{1}{W} \int_0^W \log_2 \left(1 + \frac{\rho |\hat{s}(f)|^2}{T} \right) df \text{ [bps/Hz]}. \quad (15)$$

When the RRC pulse is used, (14) may be simplified further by using the closed-form expression (12) for the folded-spectrum.

B. Normal Approximation

We now present a normal approximation of MCCR for the considered FTN signaling. This generalizes the normal approximation derived in [13] for real-valued FTN signaling with $\tau = \tau_0$ to complex baseband FTN with arbitrary $\tau < 1$.

Proposition 1 (normal approximation): Assume the constant power constraint, $|\tilde{x}_n|^2 = 1$ for all n , and a fixed $\tau < 1$. A normal approximation of MCCR for the N -parallel Gaussian channel model of FTN signaling at TBP Ω with average BLER P_e is given by

$$R_{NA}(\tau) = C_{NA}(\tau) - \sqrt{\frac{V_{NA}(\tau)}{\Omega}} \log_2(e) Q^{-1}(P_e) + \frac{\log_2(\Omega)}{2\Omega} \text{ [bps/Hz]}, \quad (16)$$

where Q^{-1} denotes the inverse Q -function (i.e., inverse function of the complementary Gaussian cumulative distribution function) and

$$\begin{aligned} C_{NA}(\tau) &\triangleq \frac{1}{\Omega} \sum_{n=0}^{N-1} \log_2 \left(1 + \frac{1}{\sigma_n^2} \right), \\ V_{NA}(\tau) &\triangleq \frac{1}{\Omega} \sum_{n=0}^{N-1} \left(1 - \frac{1}{(1 + 1/\sigma_n^2)^2} \right) \end{aligned} \quad (17)$$

are the FBL approximations to the channel capacity and the channel dispersion, respectively, where $\sigma_n^2 = (\rho\tau\lambda_n)^{-1}$. In terms of BLER P_e , the normal approximation may be also stated as the Q -function:

$$P_e \approx Q \left(\frac{C_{NA}(\tau) - R_{NA}(\tau) + \log_2(\Omega)/(2\Omega)}{\sqrt{V_{NA}(\tau)/\Omega} \cdot \log_2(e)} \right). \quad (18)$$

Proof of the proposition involves asymptotic expansion of a converse bound for FTN signaling and is shown later in Section III-D. Here, in lieu of the complete proof, we present a simpler (but partial) proof of the proposition that recovers (16) up to the second-order term. First consider real, N -parallel AWGN channels with m real-valued symbols sent in each channel. The n^{th} channel output has the form $\mathbf{r}_n = \mathbf{a}_n + \mathbf{w}_n$, where each vector has length m , the channel input \mathbf{a}_n is assumed to have fixed power, i.e., $\frac{1}{m} \|\mathbf{a}_n\|^2 = P_n$, and the additive Gaussian noise $\mathbf{w}_n \sim \mathcal{N}(\mathbf{0}, \omega_n^2 \mathbf{I})$ is independent of \mathbf{a}_n . SNR in n^{th} channel is $SNR_n = P_n/\omega_n^2$. A normal approximation of this N real-valued

parallel Gaussian channel in bits per channel use is given by [[21], Theorem 10]

$$R_N = C_N - \sqrt{\frac{V_N}{mN}} \log_2(e) Q^{-1}(P_e) + \frac{\log_2(mN)}{2mN},$$

where C_N and V_N are

$$C_N = \frac{1}{N} \sum_{n=0}^{N-1} \frac{1}{2} \log_2(1 + SNR_n) \quad \text{and}$$

$$V_N = \frac{1}{N} \sum_{n=0}^{N-1} \frac{1}{2} \left(1 - \frac{1}{(1 + SNR_n)^2} \right).$$

Coding over the complex channels may be seen as coding over real channels using a blocklength of $2N$ [22]. First, express the FTN channel output (9) as

$$\tilde{\mathbf{y}} = \tilde{\mathbf{y}}_{\text{Re}} + j\tilde{\mathbf{y}}_{\text{Im}} = (\tilde{\mathbf{x}}_{\text{Re}} + \tilde{\mathbf{z}}_{\text{Re}}) + j(\tilde{\mathbf{x}}_{\text{Im}} + \tilde{\mathbf{z}}_{\text{Im}}),$$

where the subscripts Re and Im denote the real and imaginary components, respectively, of the corresponding vectors. Rearranging,

$$[\tilde{\mathbf{y}}_{\text{Re}}, \tilde{\mathbf{y}}_{\text{Im}}] = [\tilde{\mathbf{x}}_{\text{Re}}, \tilde{\mathbf{x}}_{\text{Im}}] + [\tilde{\mathbf{z}}_{\text{Re}}, \tilde{\mathbf{z}}_{\text{Im}}],$$

where $[\tilde{\mathbf{y}}_{\text{Re}}, \tilde{\mathbf{y}}_{\text{Im}}]$ is the $N \times 2$ matrix formed by concatenating $\tilde{\mathbf{y}}_{\text{Re}}$ and $\tilde{\mathbf{y}}_{\text{Im}}$. We may treat the two symbols in each row being transmitted in one of the N -parallel channels. Note that the real and imaginary noise components, $\tilde{\mathbf{z}}_{\text{Re}}$ and $\tilde{\mathbf{z}}_{\text{Im}}$, are independent due to the circular symmetry of the additive complex Gaussian noise and the variances of the individual entries are halved from that of the complex noise counterpart $\tilde{\mathbf{z}}$. Setting $m = 2$, $SNR_n = 1/\sigma_n^2$ (due to $P_n = 1/2$ for the constant input power and $\omega_n^2 = \sigma_n^2/2$) for FTN, doubling the rates by noting that two (real-valued) symbols are sent for every one complex symbol, and changing the units to bps/Hz by noting that N FTN symbols are sent per one TBP Ω , we obtain the expression (16) up to the second-order term.

Remark 1: As $\Omega \rightarrow \infty$ for any fixed $\tau < 1$, $C_{NA}(\tau) \rightarrow C_{FTN}(\tau)$ and $R_{NA}(\tau) \rightarrow C_{FTN}(\tau)$, thus the normal approximation is asymptotically tight.

Remark 2: Similarly, as $\Omega \rightarrow \infty$ for any fixed $\tau < 1$ and using the asymptotic eigenvalue distribution (10),

$$V_{NA}(\tau) \rightarrow \frac{1}{2W} \int_0^{1/(\tau T)} \left(1 - \frac{1}{\left(1 + \frac{\rho}{T} \hat{s}_{\text{folded}}(f)\right)^2} \right) df,$$

which agrees with the channel dispersion term of *i.i.d.* FTN derived in [13] when $\tau = \tau_0$ and data symbols are real-valued.

In the literature, the normal approximation is known to yield a simple, yet remarkably tight, approximation to MCCR (or BLER) in AWGN channels [14]. However, it may be inaccurate for Ω small ($\Omega \lesssim 100$) or when the selected rate is significantly smaller than the capacity. For these reasons, converse and achievability bounds which provide true upper and lower bounds, respectively, of MCCR are often necessary.

These bounds are investigated next.

C. Converse Upper-Bound

We consider the Polyanskiy-Poor-Verdú (PPV) meta-converse bound [14], which is one of the tightest bounds available for AWGN channels. The PPV meta-converse is based on a binary hypothesis test between two hypotheses about a given observation pair (\mathbf{x}, \mathbf{y}) being distributed as either

$$H_1 : (\mathbf{x}, \mathbf{y}) \sim p_{y|x} p_x \quad \text{or} \quad H_0 : (\mathbf{x}, \mathbf{y}) \sim q_y p_x$$

for some choice of the probability density function (PDF) q_y . The Neyman-Pearson test is a log-likelihood ratio test given by

$$\Lambda(\mathbf{x}, \mathbf{y}) = \frac{1}{N} \ln \frac{p_{y|x}(\mathbf{y}|\mathbf{x})^{H_1}}{q_y(\mathbf{y})^{H_0}} \underset{H_0}{\gtrsim} \lambda,$$

for some λ . The two associated probability of errors (i.e., the missed detection (MD) and the false alarm (FA) probabilities) are, for a given \mathbf{x}

$$P_{MD}(\mathbf{x}, \lambda) = P[\Lambda(\mathbf{x}, \mathbf{y}) < \lambda | H_1, \mathbf{x}]$$

$$P_{FA}(\mathbf{x}, \lambda) = P[\Lambda(\mathbf{x}, \mathbf{y}) > \lambda | H_0, \mathbf{x}]$$

and for a given codebook \mathcal{C} ,

$$P_{MD}(\lambda) = \sum_{\mathbf{x} \in \mathcal{C}} P_{MD}(\mathbf{x}, \lambda) p_x(\mathbf{x})$$

$$P_{FA}(\lambda) = \sum_{\mathbf{x} \in \mathcal{C}} P_{FA}(\mathbf{x}, \lambda) p_x(\mathbf{x}).$$

Using the notations above, one version of the PPV meta-converse can be stated as follows (see [[14], Theorem 27] for more general version of the theorem).

Theorem 1 (PPV meta-converse [14], [21]): Assume that $p_x(\mathbf{x}) = 1/M$ (equally likely message) for all $\mathbf{x} \in \mathcal{C}$ and P_e is the average BLER. If q_y is chosen in such a way that both MD and FA probabilities are independent of \mathbf{x} , then for a fixed P_e , the code rate R is upper-bounded as

$$R \leq -\frac{1}{N} \log_2 P_{FA}(\lambda) \quad [\text{bpcu}],$$

where λ satisfies $P_{MD}(\lambda) = P_e$.

Proof: See [[14], Theorem 28]. ■

The PPV meta-converse for the considered FTN signaling is given in the following theorem.

Theorem 2 (meta-converse for FTN): Let $\mathcal{X}^2(k, \nu)$ denote the complex noncentral chi-square distribution with degree of freedom k and noncentrality parameter ν . Let $U_n \sim \mathcal{X}^2(1, 1 + \sigma_n^2)$ and $V_n \sim \mathcal{X}^2(1, \sigma_n^2)$ be two random variables for $n = 0, 1, \dots, N-1$, both independent in n . The PPV meta-converse for the FTN channel model, $\tilde{\mathbf{y}} = \tilde{\mathbf{x}} + \tilde{\mathbf{z}}$, under the constant power constraint, $|\tilde{x}_n|^2 = 1$ for all n , is given by

$$R \leq -\frac{1}{\Omega} \log_2 P \left[\frac{1}{N} \sum_{n=0}^{N-1} \frac{1}{\sigma_n^2} U_n < \lambda \right] \quad [\text{bps/Hz}], \quad (19)$$

where λ is chosen to satisfy

$$P_e = P \left[\frac{1}{N} \sum_{n=0}^{N-1} \frac{1}{1 + \sigma_n^2} V_n > \lambda \right]. \quad (20)$$

Proof: For the N -parallel Gaussian channel model, we have $p_{\tilde{y}|\tilde{x}}(\tilde{\mathbf{y}}|\tilde{\mathbf{x}}) = \prod_{n=0}^{N-1} p_{\tilde{y}_n|\tilde{x}_n}(\tilde{y}_n|\tilde{x}_n) = \prod_{n=0}^{N-1} \frac{1}{\pi\sigma_n^2} \exp\left(-\frac{1}{\sigma_n^2}|\tilde{y}_n - \tilde{x}_n|^2\right)$. A judicious choice for $q_{\tilde{y}}(\tilde{\mathbf{y}})$ is the capacity-achieving output distribution, i.e., $\tilde{\mathbf{y}} \sim \mathcal{CN}(\mathbf{0}, \mathbf{I} + \mathbf{D})$, where \mathbf{D} is a diagonal covariance matrix of $\tilde{\mathbf{z}}$ with n^{th} diagonal entry equal to σ_n^2 . Thus,

$$q_{\tilde{y}}(\tilde{\mathbf{y}}) = \prod_{n=0}^{N-1} q_{\tilde{y}_n}(\tilde{y}_n) = \prod_{n=0}^{N-1} \frac{1}{\pi(1+\sigma_n^2)} \exp\left(-\frac{1}{(1+\sigma_n^2)}|\tilde{y}_n|^2\right).$$

Let *mismatched* information density be defined as

$$i(\tilde{x}_n; \tilde{y}_n) \triangleq \ln \left(\frac{p_{\tilde{y}_n|\tilde{x}_n}(\tilde{y}_n|\tilde{x}_n)}{q_{\tilde{y}_n}(\tilde{y}_n)} \right).$$

It can be simplified as

$$i(\tilde{x}_n; \tilde{y}_n) = \ln \left(1 + \frac{1}{\sigma_n^2} \right) - \frac{|\tilde{y}_n - (1 + \sigma_n^2)\tilde{x}_n|^2}{\sigma_n^2(1 + \sigma_n^2)} + |\tilde{x}_n|^2. \quad (21)$$

The FA probability is then

$$\begin{aligned} P_{FA}(\tilde{\mathbf{x}}, \lambda) &= P \left[\frac{1}{N} \sum_{n=0}^{N-1} i(\tilde{x}_n; \tilde{y}_n) > \lambda \mid H_0, \tilde{\mathbf{x}} \right] \\ &= P \left[\frac{1}{N} \sum_{n=0}^{N-1} \ln \left(1 + \frac{1}{\sigma_n^2} \right) - \frac{1}{N} \sum_{n=0}^{N-1} \frac{|\tilde{y}_n - (1 + \sigma_n^2)\tilde{x}_n|^2}{\sigma_n^2(1 + \sigma_n^2)} + 1 > \lambda \mid H_0, \tilde{\mathbf{x}} \right] \end{aligned}$$

due to $|\tilde{x}_n|^2 = 1$. Under the hypothesis H_0 , $\tilde{y}_n \sim q_{\tilde{y}_n}(\tilde{y}_n) = \mathcal{CN}(0, 1 + \sigma_n^2)$ and

$$\left| \frac{\tilde{y}_n - (1 + \sigma_n^2)\tilde{x}_n}{\sqrt{1 + \sigma_n^2}} \right|^2 \sim \mathcal{X}^2(1, 1 + \sigma_n^2), \quad (22)$$

where the noncentrality parameter, $1 + \sigma_n^2$, is obtained by the assumption $|\tilde{x}_n|^2 = 1$. Defining U_n as (22), the FA probability may be simplified as

$$P_{FA}(\tilde{\mathbf{x}}, \lambda) = P \left[\frac{1}{N} \sum_{n=0}^{N-1} \frac{1}{\sigma_n^2} U_n < -\lambda + 1 + \sum_{n=0}^{N-1} \ln \left(1 + \frac{1}{\sigma_n^2} \right) \right].$$

The above is independent of $\tilde{\mathbf{x}}$, hence $P_{FA}(\tilde{\mathbf{x}}, \lambda) = P_{FA}(\lambda)$.

As for the MD probability, note that under the hypothesis H_1 , $\tilde{y}_n \sim p_{\tilde{y}_n|\tilde{x}_n}(\tilde{y}_n|\tilde{x}_n) = \mathcal{CN}(\tilde{x}_n, \sigma_n^2)$ and

$$\left| \frac{\tilde{y}_n - (1 + \sigma_n^2)\tilde{x}_n}{\sqrt{\sigma_n^2}} \right|^2 \sim \mathcal{X}^2(1, \sigma_n^2), \quad (23)$$

where the noncentrality parameter is again obtained by the assumption $|\tilde{x}_n|^2 = 1$. Defining V_n as (23), the MD probability may be simplified as

$$\begin{aligned} P_{MD}(\tilde{\mathbf{x}}, \lambda) &= P \left[\frac{1}{N} \sum_{n=0}^{N-1} i(\tilde{x}_n; \tilde{y}_n) < \lambda \mid H_1, \tilde{\mathbf{x}} \right] \\ &= P \left[\frac{1}{N} \sum_{n=0}^{N-1} \frac{1}{1 + \sigma_n^2} V_n > -\lambda + 1 + \sum_{n=0}^{N-1} \ln \left(1 + \frac{1}{\sigma_n^2} \right) \right]. \end{aligned}$$

Again, the MD probability is independent of $\tilde{\mathbf{x}}$, hence $P_{MD}(\tilde{\mathbf{x}}, \lambda) = P_{MD}(\lambda)$. Finally, without loss of generality, we may redefine λ as the terms appearing on the RHS of the inequalities in both P_{FA} and P_{MD} . Substituting these into Theorem 1 and changing the units yields the desired result. ■

Evaluating the meta-converse bounds directly is difficult, because PDF of the weighted sum of $\mathcal{X}^2(1, \nu)$ is unavailable in a closed form and the tail probabilities can get smaller than typical computing precision limit, thus making the Monte-Carlo methods infeasible. Fortunately, one may accurately approximate these bounds using methods such as the saddlepoint approximations [23], [24]. Appendix A shows an approximation of the meta-converse bound using the method in [24].

D. Asymptotic Expansion of the Meta-Converse Bound and Proof of Proposition 1

We now investigate an asymptotic expansion of the meta-converse bound for FTN signaling using the Berry-Esseen theorem. This recovers the normal approximation $R_{NA}(\tau)$ and proves Proposition 1.

Under the settings of Theorem 2, we first relax the meta-converse bound using the following inequality on the FA probability [[14], eq. (106)]:

$$P_{FA}(\lambda) \geq \sup_{\gamma > 0} \left\{ e^{-N\gamma} \left((1 - P_e) - (1 - P_{MD}(\gamma)) \right) \right\}.$$

This bound assumes that the FA and MD probabilities are independent of the transmitted codeword. Applying the above bound to the PPV meta-converse theorem results in a generalized version of Verdú-Han converse bound [25], [26]:

$$R \leq \inf_{\gamma > 0} \left\{ \gamma \log_2(e) - \frac{1}{N} \log_2(P_{MD}(\gamma) - P_e) \right\} \text{ [bpcu]}. \quad (24)$$

For the FTN channel, recall that the MD probability is given by

$$P_{MD}(\gamma) = P \left[\sum_{n=0}^{N-1} i(\tilde{x}_n; \tilde{y}_n) \leq N\gamma \mid H_1, \tilde{\mathbf{x}} \right],$$

where the mismatched information density $i(\tilde{x}_n; \tilde{y}_n)$ is given by (21) for the FTN channel. We will need the first three moments of $i(\tilde{x}_n; \tilde{y}_n)$, which are given in the lemma below.

Lemma 2 (moments of mismatched information density): Let $|\tilde{x}_n| = 1$. The mean and the variance of the mismatched information density $i(\tilde{x}_n; \tilde{y}_n)$ under $\tilde{y}_n \sim p_{\tilde{y}_n|\tilde{x}_n} = \mathcal{CN}(\tilde{x}_n, \sigma_n^2)$

and for a fixed \tilde{x}_n are

$$\begin{aligned} c_n &\triangleq \mathbb{E}_{\tilde{y}_n} [i(\tilde{x}_n; \tilde{y}_n)] = \ln(1 + 1/\sigma_n^2), \\ v_n &\triangleq \text{var}_{\tilde{y}_n} [i(\tilde{x}_n; \tilde{y}_n)] = 1 - \frac{1}{(1 + 1/\sigma_n^2)^2}. \end{aligned} \quad (25)$$

The third absolute central moment, $\theta_n \triangleq \mathbb{E}_{\tilde{y}_n} [|i(\tilde{x}_n; \tilde{y}_n) - c_n|^3]$, can be bounded as

$$v_n^{3/2} \leq \theta_n \leq \sqrt{27} v_n^{3/2}. \quad (26)$$

Proof: Both c_n and v_n are straightforward. θ_n may be bound using the power norm inequality:

$$\left(\mathbb{E}_{\tilde{y}_n} [|i(\tilde{x}_n; \tilde{y}_n) - c_n|^2] \right)^{1/2} \leq \theta_n^{1/3} \leq \left(\mathbb{E}_{\tilde{y}_n} [|i(\tilde{x}_n; \tilde{y}_n) - c_n|^4] \right)^{1/4}.$$

The proof is then complete by noting that the fourth central moment may be upper-bounded by $9v_n^2$. ■

Corollary 1: Let $B \triangleq (\frac{1}{\Omega} \sum_n \theta_n) / (\frac{1}{\Omega} \sum_n v_n)^{3/2}$. As TBP Ω grows, B behaves as $\mathcal{O}(1)$ in the FTN channel.

We now apply the Berry-Esseen central limit theorem (CLT) to lower bound the MD probability in terms of the first three moments of the mismatched information density. This yields,

$$P_{MD}(\gamma) \geq Q \left(-\frac{N\gamma - \sum_n c_n}{\sqrt{\sum_n v_n}} \right) - \frac{B}{\sqrt{\Omega}}.$$

Instead of optimizing over γ , we choose (sub-optimally)

$$N\gamma = \sum_n c_n - \sqrt{\sum_n v_n} Q^{-1}(P_e + 2B/\sqrt{\Omega}),$$

which results in the lowerbound:

$$P_{MD}(\gamma) \geq P_e + B/\sqrt{\Omega}.$$

Substituting the above into the Verdú-Han bound (24) and converting the units to bps/Hz (by noting N FTN symbols are sent per Ω s/Hz), we obtain:

$$\begin{aligned} R &\leq C_{NA} - \sqrt{\frac{V_{NA}}{\Omega}} \log_2(e) Q^{-1} \left(P_e + \frac{2B}{\sqrt{\Omega}} \right) - \frac{1}{\Omega} \log_2 \left(\frac{B}{\sqrt{\Omega}} \right) \\ &= C_{NA} - \sqrt{\frac{V_{NA}}{\Omega}} \log_2(e) Q^{-1}(P_e) + \frac{\log_2(\Omega)}{2\Omega} + \mathcal{O}(1/\Omega), \end{aligned}$$

where in the last step, we used the Taylor series expansion on $Q^{-1}(a+b) \approx a + \frac{Q^{-1(a)}}{1!} b + \frac{Q^{-1(2)(a)}}{2!} b^2 + \dots$ and collected all terms of order $1/\Omega$ into $\mathcal{O}(1/\Omega)$. This proves Proposition 1 and confirms that R_{NA} is accurate up to $\mathcal{O}(1/\Omega)$.

E. Achievability Lower-Bound

The random-coding union (RCU) achievability bound [14] is based on Shannon's random coding argument.

Theorem 3 (RCU [14]): Let a (M, N) code for a channel $p_{y|x}$ consists of M codewords of length N with the rate

$R = \frac{1}{N} \log_2 M$ bits per channel use. Then for every M and N , there exists a code whose error probability is upper-bounded by

$$P_e \leq \mathbb{E}_{\mathbf{x}, \mathbf{y}} \left[\min \{ 1, (M-1) g(\mathbf{x}, \mathbf{y}) \} \right] \quad (27)$$

with $\mathbf{y} \sim p_{y|x}$, $\mathbf{x} \sim p_x$, where $g(\mathbf{x}, \mathbf{y})$ is the pairwise error probability defined by

$$g(\mathbf{x}, \mathbf{y}) \triangleq P \left[p_{y|x}(\mathbf{y}|\mathbf{w}) \geq p_{y|x}(\mathbf{y}|\mathbf{x}) \mid \mathbf{x}, \mathbf{y} \right]$$

for $\mathbf{w} \sim p_x$ that is independent of \mathbf{x} . In terms of the *matched* information density $i(\mathbf{x}; \mathbf{y}) \triangleq \ln(p_{y|x}(\mathbf{y}|\mathbf{x})/p_y(\mathbf{y}))$, $g(\mathbf{x}, \mathbf{y})$ may be also expressed as

$$g(\mathbf{x}, \mathbf{y}) = P \left[i(\mathbf{w}; \mathbf{y}) \geq i(\mathbf{x}; \mathbf{y}) \mid \mathbf{x}, \mathbf{y} \right]. \quad (28)$$

Proof: See [[14], Theorem 16]. ■

While the RCU bound works for arbitrary input distributions, we consider the average power constraint $\mathbb{E}\{|\tilde{x}_n|^2\} = 1$ as it allows us to choose the capacity-achieving complex normal distribution for the input which greatly simplifies the bound. It should be noted that the both the average power constraint and the constant power constraint, considered for the meta-converse bound, yield the same PSD for the FTN signal that is fixed regardless of τ . The RCU bound for the considered FTN signaling is given in the following theorem.

Theorem 4 (RCU for FTN): Let $\chi^2(k, \nu)$ denote the complex noncentral chi-square distribution. Let $V_n(\tilde{y}_n) \sim \chi^2(1, |\tilde{y}_n|^2)$ for $\tilde{y}_n \in \mathbb{C}$ be independent in $n = 0, 1, \dots, N-1$. For some target rate R in bps/Hz, the RCU bound for the FTN channel model, $\tilde{\mathbf{y}} = \tilde{\mathbf{x}} + \tilde{\mathbf{z}}$, under the average input power constraint, $\mathbb{E}\{|\tilde{x}_n|^2\} = 1$ for all n , is given by

$$\boxed{P_e \leq \mathbb{E}_{\tilde{\mathbf{x}}, \tilde{\mathbf{y}}} \left[\min \left\{ 1, \left(2^{\Omega R} - 1 \right) \cdot P \left[\sum_{n=0}^{N-1} \frac{1}{\sigma_n^2} V_n(\tilde{y}_n) \leq \mu(\tilde{\mathbf{x}}, \tilde{\mathbf{y}}) \mid \tilde{\mathbf{x}}, \tilde{\mathbf{y}} \right] \right\} \right]}, \quad (29)$$

where $\tilde{\mathbf{x}} \sim \mathcal{CN}(\mathbf{0}, \mathbf{I})$ and $\tilde{\mathbf{y}} = \tilde{\mathbf{x}} + \tilde{\mathbf{z}}$ with $\tilde{\mathbf{z}} \sim \mathcal{CN}(\mathbf{0}, \mathbf{D})$ having covariance $\mathbf{D} = \text{diag}(\sigma_0^2, \dots, \sigma_{N-1}^2)$, and $\mu(\tilde{\mathbf{x}}, \tilde{\mathbf{y}}) \triangleq \sum_{n=0}^{N-1} \frac{1}{\sigma_n^2} |\tilde{x}_n - \tilde{y}_n|^2 = (\tilde{\mathbf{x}} - \tilde{\mathbf{y}})^\dagger \mathbf{D}^{-1} (\tilde{\mathbf{x}} - \tilde{\mathbf{y}})$.

Proof: The matched information density between the input symbols $\tilde{\mathbf{x}}$ and the FTN channel output $\tilde{\mathbf{y}}$, when $\tilde{\mathbf{y}} \sim \mathcal{CN}(\mathbf{0}, \mathbf{I} + \mathbf{D})$, may be expressed as

$$i(\tilde{\mathbf{x}}; \tilde{\mathbf{y}}) = \sum_{n=0}^{N-1} i(\tilde{x}_n; \tilde{y}_n), \quad (30)$$

where

$$i(\tilde{x}_n; \tilde{y}_n) \triangleq \ln \left(\frac{P(\tilde{y}_n | \tilde{x}_n)}{P(\tilde{y}_n)} \right)$$

$$= \ln \left(1 + \frac{1}{\sigma_n^2} \right) - \frac{|\tilde{y}_n - \tilde{x}_n|^2}{\sigma_n^2} + \frac{|\tilde{y}_n|^2}{1 + \sigma_n^2}. \quad (31)$$

To see this, first note that $\tilde{\mathbf{y}}|\tilde{\mathbf{x}} \sim \mathcal{CN}(\tilde{\mathbf{x}}, \mathbf{D})$ and hence $p(\tilde{\mathbf{y}}|\tilde{\mathbf{x}}) = \prod_n p(\tilde{y}_n|\tilde{x}_n)$ and $p(\tilde{\mathbf{y}}) = \prod_n p(\tilde{y}_n)$, and (30) follows immediately. Substituting the corresponding complex normal PDFs and simplifying yields (31). Then, $g(\tilde{\mathbf{x}}, \tilde{\mathbf{y}})$ from (28) simplifies to:

$$\begin{aligned} g(\tilde{\mathbf{x}}, \tilde{\mathbf{y}}) &= P \left[i(\mathbf{w}; \tilde{\mathbf{y}}) \geq i(\tilde{\mathbf{x}}; \tilde{\mathbf{y}}) \mid \tilde{\mathbf{x}}, \tilde{\mathbf{y}} \right] \\ &= P \left[\sum_{n=0}^{N-1} \frac{1}{\sigma_n^2} |w_n - \tilde{y}_n|^2 \leq \sum_{n=0}^{N-1} \frac{1}{\sigma_n^2} |\tilde{x}_n - \tilde{y}_n|^2 \mid \tilde{\mathbf{x}}, \tilde{\mathbf{y}} \right] \end{aligned} \quad (32)$$

Finally, $|w_n - \tilde{y}_n|^2 \sim \mathcal{X}^2(1, |\tilde{y}_n|^2)$ when $\mathbf{w} \sim p_{\tilde{\mathbf{x}}} = \mathcal{CN}(0, \mathbf{I})$.

This completes the proof of Theorem 4. \blacksquare

As with the meta-converse bound, computing the RCU bound is numerically challenging for moderate to large values of Ω and SNR (due to the cumulative distribution function (CDF) in (29) being small and often below the dynamic range of the computing precision). Similar to the meta-converse bound, we can accurately approximate the RCU bound (e.g., using methods that approximate CDF of sum of independent random variables – see Appendix A).

It is possible to apply an asymptotic expansion on the RCU bound, similar to the expansion applied to the meta-converse bound in Section III.D. This yields

$$R_{RCU} = C_{NA} - \sqrt{\frac{V_{RCU}}{\Omega}} \log_2(e) \mathcal{Q}^{-1}(P_e) + \mathcal{O}(1/\Omega),$$

where $V_{RCU} \triangleq 2/(1 + \sigma_n^2)$. We omit the proof and instead refer the reader to the steps outlined in [26] using the Berry-Esseen theorem. Comparing this expansion to the normal approximation R_{NA} from Proposition 1, we note that the second order term is larger now due to $V_{RCU} = V_{NA} + (1 + \sigma_n^2)^{-2} > V_{NA}$ and the third order term from R_{NA} , i.e., $\log_2(\Omega)/(2\Omega)$, is missing and instead contained in $\mathcal{O}(1/\Omega)$. The larger second order term is a consequence of using *i.i.d.* Gaussian symbols in deriving the RCU bound (which is a suboptimal choice in the FBL regime – see [27] for a similar observation). These imply that the asymptotic expansion of RCU with *i.i.d.* Gaussian symbols is in general less tight than that of the meta-converse bound. Nevertheless, in our numerical results, the RCU bound is shown to provide tractable and reasonably tight lower-bound to MCCR in the FBL regime in most scenarios of interests.

IV. DISCUSSION ON THE MERITS OF FTN IN THE FBL REGIME

We now discuss the potential merits of FTN signaling in the FBL regime. For the clarity of the discussion, we assume throughout that RRC pulse with roll-off factor β and define $\tau_0 = 1/(1+\beta)$, but similar conclusions can be made for any

bandlimited, T -orthogonal modulating pulses with τ_0 defined as $1/(2WT)$, where W is the bandwidth of the pulse shape.

A. Case $\tau_0 \leq \tau < 1$

When $\tau_0 \leq \tau < 1$, the capacity continually increases with decreasing τ , due to the bounds of the integral in $C_{FTN}(\tau)$ (14) expanding as $1/(\tau T)$ and the integrand being nonzero over the integration range. The capacity shows that FTN can regain the penalty from using practical pulse shaping. Since the ideal sinc pulse has greater penalty in the FBL regime from having slowly decaying tails and high sensitivity to synchronization mismatch, the benefit becomes more significant when packets are short.

The capacity may be approached in the asymptotic blocklength regime. In the FBL regime (with practical BLER target), MCCR of FTN can also increase as τ is decreased. Fig. 4 shows MCCR of FTN signaling along with the meta-converse upper-bound, the RCU lower-bound, and the normal approximation at SNR $\rho = \{10 \text{ dB}, 30 \text{ dB}\}$ and $P_e = 10^{-3}$. The RRC pulse with $\beta = 0.5$ is assumed throughout, which leads to $\tau_0 = 1/(1+\beta) = 2/3$. We observe that both the capacity and MCCR increase as τ is decreased for all TBP and at both low and high SNRs.

Fig. 5 shows BLER P_e versus SNR ρ at TBP $\Omega = 100$, when the target rate is set as the capacity of the Nyquist rate system at $\rho = 30 \text{ dB}$, i.e., $C_{FTN}(1) = 6.646 \text{ bps/Hz}$. As τ is decreased, BLER decreases at each SNR, or equivalently, SNR required to reach the same BLER decreases for each target rate.

The degree with which MCCR increases beyond the rate of Nyquist rate signaling can be observed in Fig. 6, which plots the percentage gain $(R_{NA}(\tau) - R_{NA}(1))/R_{NA}(1)$ versus τ , at $\Omega = \{50, 100, 300\}$ and $\beta = \{0.1, 0.5, 0.9\}$. The channel SNR $\rho = 40 \text{ dB}$ (demonstrating high SNR) and $P_e = 10^{-3}$ are considered. For $\tau \geq \tau_0$, the percentage gain scales up almost linearly as τ decreases and plateaus out near 10%, 40% and 70% for $\beta = 0.1, 0.5$, and 0.9, respectively. Also, comparing between different TBPs, the percentage gain is about the same at all TBPs for all $\tau > \tau_0$, except when τ is near τ_0 there are more gains at smaller TBP ($= 50$).

These observations imply that FTN signaling can provide higher rates for fixed BLER (or equivalently, lower BLER for fixed rates) in any blocklength and any channel SNR. In the case of URLLC applications, the ability of FTN to reduce BLER (thus improving the reliability) for fixed transmission rates may be of greater interest, while in other applications where more throughput is desired under tight transmission time window and confined bandwidth, the ability of FTN to increase the spectral efficiency may be its main draw.

B. Case $\tau < \tau_0$

In the case of $\tau < \tau_0$, there is no capacity benefit to signaling below τ_0 in the asymptotic blocklength regime. In contrast, in the FBL regime, MCCR of FTN can further increase by signaling below τ_0 . Fig. 7 shows MCCR of FTN when $\tau = \{\tau_0, \tau_0/2\}$, $\rho = \{40 \text{ dB}, 50 \text{ dB}\}$, $\beta = 0.5$, and the target $P_e = 10^{-3}$. It can be observed that MCCR clearly increases when τ is below τ_0 , thereby reducing the gap between the channel coding rates

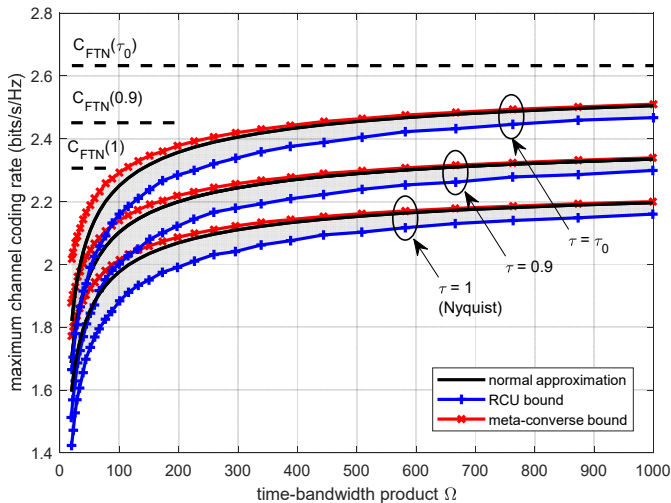
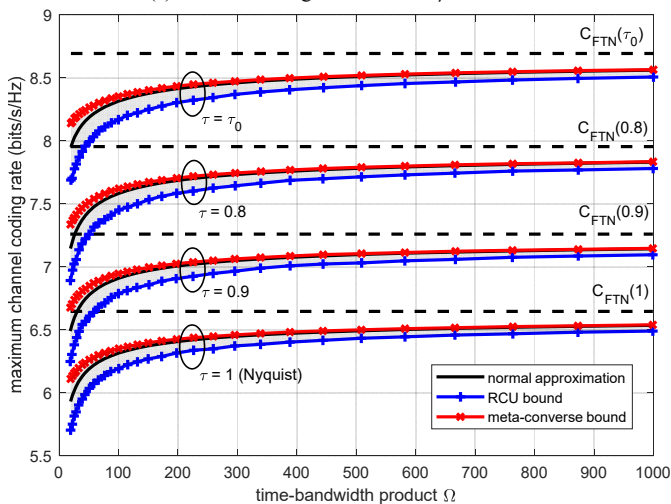
(a) Channel coding rates for SNR $\rho = 10$ dB(b) Channel coding rates for SNR $\rho = 30$ dB

Fig. 4. Demonstrating how the capacity and the channel coding rates increase with decreasing FTN acceleration factor τ (for $\tau \geq \tau_0$) at 10 dB and 30 dB SNRs in the FBL regime. Assuming that the target BLER is $P_e = 10^{-3}$ and RRC pulses with $\beta = 0.5$ is being used.

and the capacity. The gains are also seen to be comparably greater in higher SNR². These benefits are present regardless of which modulating pulses are employed including the ideal sinc pulse. We note that the gains from signaling below τ_0 are generally smaller compared to the gains from the case $\tau > \tau_0$, but they can be nonnegligible when the channel SNR is high and TBP is small.

We may also observe how the gain scales with τ and TBP when $\tau < \tau_0$ in Fig. 6. It can be observed that the FTN gain is greater at smaller TBP ($= 50$), and it takes τ strictly smaller than τ_0 to reach the maximum gain. In addition, Fig. 8 shows BLER of FTN at TBP = 100 when the target rate is $C_{FTN}(\tau_0)$ at $\rho = 50$ dB, which demonstrates that BLER decreases with τ below τ_0 ,

² In Fig. 7b, at very low TBP, MCCRs are seen to be higher than the capacity, which is possible due to allowing nonzero block error rates $P_e > 0$ in the FBL regime. We note that the strong converse of the channel coding theorem [20] has not been violated, because L transmissions of N length blocks will have the overall block error rate of $1 - (1 - P_e)^L$ across the L transmissions, which still converges to 1 as L tends to infinity for any $P_e > 0$ fixed.

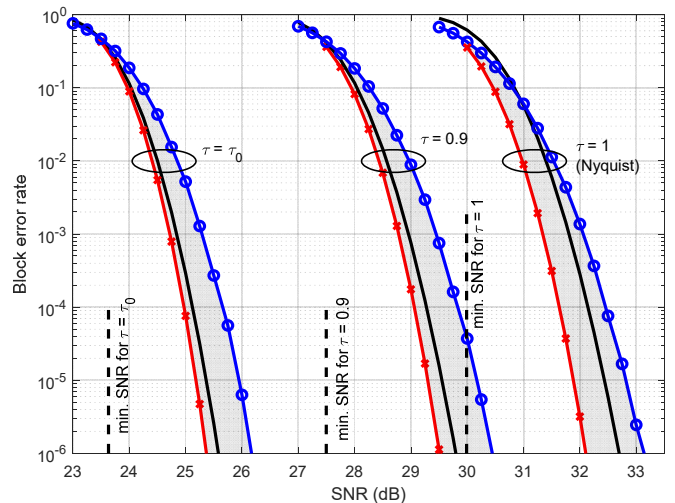


Fig. 5. Demonstrating how the minimum SNR and BLER decrease with decreasing FTN acceleration factor τ (for $\tau \geq \tau_0$) at TBP $\Omega = 100$, when the target data rate is fixed at 6.646 bps/Hz ($= C_{FTN}(1)$ at $\rho = 30$ dB). RRC pulses with $\beta = 0.5$ is being used.

hence bringing the error rates closer to the (asymptotic) minimum SNR limit. These observations imply that FTN signaling below τ_0 finds merit in the FBL regime, and in most cases it suffices to signal slightly below τ_0 to get most of the gains.

C. Signaling Dimensions and Merits to Signaling Below τ_0

The benefits of FTN signaling below τ_0 can be explained from insufficiency of Nyquist rate sampling to represent all bandlimited signals within a finite time window. If the sampling window is restricted to a finite time interval, one needs to sample above Nyquist rate to accurately specify bandlimited signals. Analogously, under a bandwidth constraint and within a finite time window, Nyquist rate signaling is insufficient to utilize all available signaling dimensions. By deliberately signaling faster, FTN allows accessing an increased number of signaling dimensions than that of Nyquist rate signaling. The gains can be directly computed from SNR of the N -parallel Gaussian channel model of FTN signaling.

Viewing from Shannon's geometric representation of signals and noise and the random-coding argument [16], FTN signaling allows choosing more codewords from the higher dimensional space of bandlimited functions within a finite time support. At high SNR, significantly more codewords may be selected from this space due to noise being smaller, and hence additional dimensions provided by FTN signaling result in a higher and more noticeable gain. We note that this gain is unique to the FBL regime, since the dimensionality of the space given by FTN and Nyquist rate signaling converge as the blocklength tends to infinity.

D. FTN with Finite Constellations

In the asymptotic blocklength regime, FTN is known to achieve the capacity with only finite (e.g., binary or BPSK) modulation symbols by taking $\tau \rightarrow 0$ [28]. Although the proof involves more advanced machinery, this result may be inferred from observing that the input distribution of the N -parallel

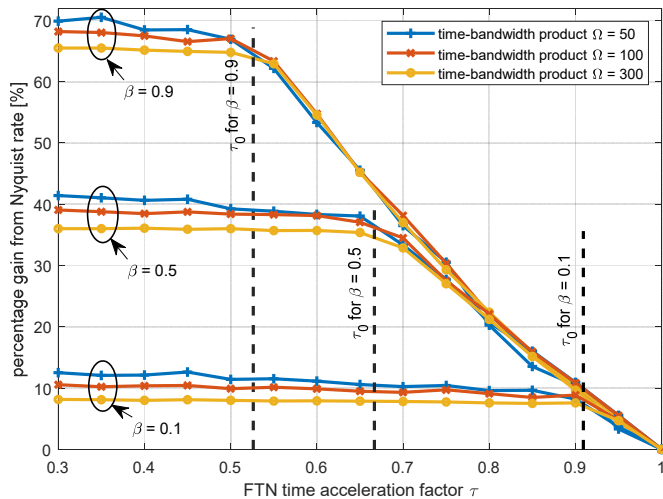


Fig. 6. Plotting percentage gain from Nyquist rate signaling: $(R_{NA}(\tau) - R_{NA}(1))/R_{NA}(1)$ versus τ at TBP $\Omega = \{50, 100, 300\}$ and roll-off factor $\beta = \{0.1, 0.5, 0.9\}$. Assuming SNR $\rho = 40$ dB and BLER $P_e = 10^{-3}$. The thresholds $\tau_0 = 1/(1+\beta)$ for each β are also annotated.

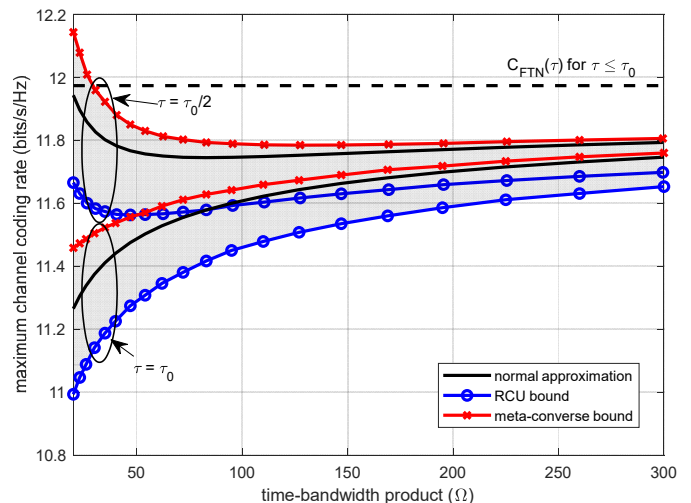
Gaussian channel of FTN approaches Gaussian due to the CLT, as $\Omega \rightarrow \infty$ and $\tau \rightarrow 0$.

Similar observations can be made in the FBL regime. We first recall that the input to the N -parallel Gaussian channel is $\tilde{\mathbf{x}} = \mathbf{U}^T \mathbf{x}$. Let its n^{th} element be denoted by $\tilde{x}_n = \mathbf{u}_n^T \mathbf{x}$ with \mathbf{u}_n being the n^{th} eigenvector of \mathbf{H} . When \mathbf{x} consists of *i.i.d.* BPSK symbols, the distribution of \tilde{x}_n can be seen to approach the standard Normal distribution as τ is decreased. This can be observed in Fig. 9, which plots the normalized histograms of $\{\tilde{x}_n\}$ (over 10^6 independent realizations) for all $n = 0, 1, \dots, N-1$ along with the standard Normal distribution as a reference. We assumed $\beta = 0.5$, $\tau = \tau_0/2$, and $\Omega = 50$. Fig. 9 suggests that for small enough τ , the distributions of $\{\tilde{x}_n\}$ are all nearly Gaussian and the presented the RCU achievability bound (which has been derived with the Gaussian input assumption) may be approached by using only finite constellation symbols.

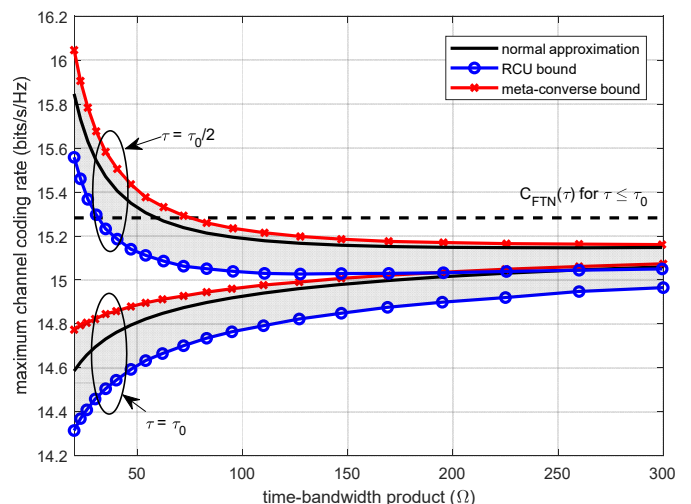
To provide further insights, we recall that FTN can increase N by lowering τ for any fixed TBP Ω . Thus, the number of independent but non-identically distributed terms being added to form $\tilde{x}_n = \mathbf{u}_n^T \mathbf{x}$ can be increased indefinitely within a fixed time window. Using the Lyapunov's condition for CLT, it can be shown that \tilde{x}_n converges to $\mathcal{N}(0,1)$ as $N \rightarrow \infty$ if, for some $p > 2$, $\lim_{N \rightarrow \infty} \|\mathbf{u}_n\|_p^p = 0$, where $\|\cdot\|_p$ denotes the p -norm. Proving the Lyapunov's condition seems difficult in our case due to the lack of closed-form expressions for the eigenvectors of \mathbf{H} , but numerical evidences (as in Fig. 9) suggest that $\{\tilde{x}_n\}$ can be all nearly Gaussian for sufficiently small τ for any fixed TBP.

V. SUMMARY AND FUTURE WORKS

By providing tight bounds on MCCR, we have identified potential merits of FTN signaling in the FBL regime. When $\tau > \tau_0$, FTN signaling was shown to have both higher capacity and higher MCCR than those of Nyquist rate signaling counterpart, when the utilized pulse shape is non-sinc. FTN was shown to



(a) Channel coding rates for SNR $\rho = 40$ dB



(b) Channel coding rates for SNR $\rho = 50$ dB

Fig. 7. Demonstrating the benefit to signaling below τ_0 in the FBL regime. Both figures assume RRC pulses with roll-off factor $\beta = 0.5$.

yield 10%, 40% and 70% higher rates than Nyquist rate signaling when the RRC pulses with roll-off factors $\beta = 0.1$, 0.5 , and 0.9 are used, respectively, and these gains can increase with higher SNR and shorter blocklength.

On the other hand, when $\tau < \tau_0$, it was shown that MCCR of FTN can continue to increase regardless of the pulse shapes (including the ideal sinc pulse), thereby reducing the gap between MCCR and the capacity of FTN. The degree to which MCCR increases is shown to be nonnegligible when the channel SNR is high and TBP is small. In other words, FTN can lower the penalty from coding over short blocklength by packing more symbols within the same TBP. This benefit is analogous to quickly reaching the maximum cruising speed while traveling a short distance.

Instead of increasing the rates for fixed BLER, FTN can alternatively lower BLER for fixed channel coding rates. This opens an avenue for using FTN to improve the reliability of short packet communications (e.g., for URLLC applications). Furthermore, we considered FTN signaling with finite symbol constellations and showed that accelerating the signaling rate has the effect of increasing the modulation order, and thus the

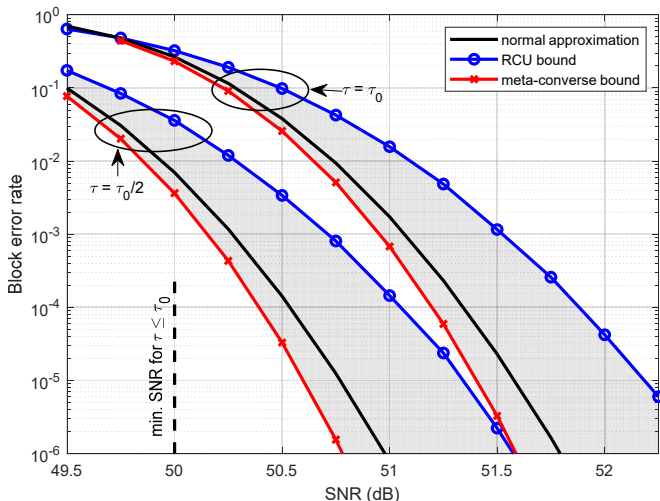


Fig. 8. Block error rates when TBP $\Omega = 100$ and the target data rate $R = 15.282$ bps/Hz ($= C_{FTN}(\tau_0)$ at $\rho = 50$ dB) when $\tau \leq \tau_0$.

presented bounds on MCCR can be approached while using finite constellation symbols with sufficiently small τ .

These results confirm that FTN signaling is fundamentally more efficient than orthogonal signaling in using the available time and frequency resources under any blocklength. Due to its fundamental nature, it is expected that its benefits universally apply to other settings not considered in this paper, including but not limited to, fading, MIMO, multiuser channels, etc.

The results from this work suggest various future research directions. First, the benefit of precoding or non-uniform power allocation can be quantified in the FBL regime. While [13] analyzed the normal approximation for non-*i.i.d.* FTN, tight lower- and upper-bounds of MCCR are missing and need to be accompanied with appropriate power spectral analysis (such as in [29]) to avoid possible spectral broadening for precoding in FTN [17]. Second, pulse shapes may be designed specifically for short packet communications. For the sake of simplicity, the MCCR analysis in this work did not account for the tail lengths of the pulse shapes but taking it into account would have shown even greater gains from using FTN signaling in the FBL regime. Third, FTN coding designs that can perform close to the presented MCCR can be considered. There are some recent works in this regard (e.g., [30], [31]). However, most of the prior literature on FTN system designs focus on long blocklength and comparison to MCCR are missing. Furthermore, the FTN receivers for the FBL regime will need to be operating under tight latency requirements, meaning that either low-complexity equalizers or precoding designs that can pre-compensate ISI to relieve some of the receiver operations may be desired. Lastly, extensions to packing in both time and frequency domains (e.g., SEFDM or multicarrier-FTN [32], [33]) and more realistic channels (e.g., fading or MIMO [34]) can be considered in the FBL regime.

APPENDIX A

APPROXIMATION OF FTN META-CONVERSE AND RCU BOUNDS

Consider a linear combination $Y = \sum_{n=0}^{N-1} X_n$, where X_n with PDF $f_{X_n}(x)$ are independent but not necessarily

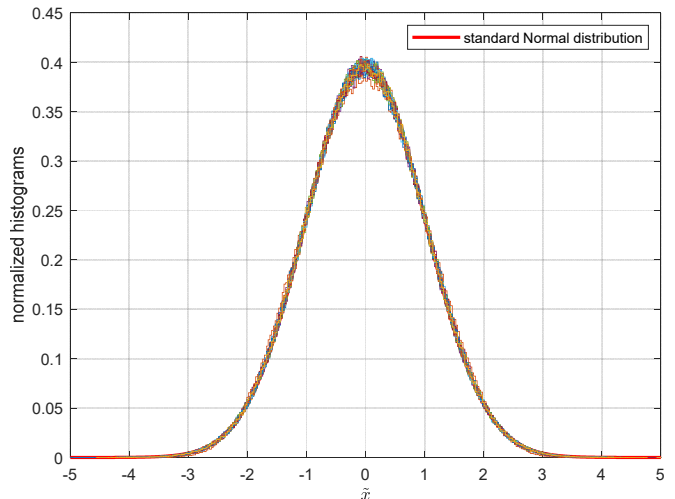


Fig. 9. Plotting normalized histograms of the input $\tilde{x}_n = \mathbf{u}_n^T \mathbf{x}$, for $n = 0, 1, \dots, N-1$, when the data symbols \mathbf{x} are binary. 10^6 samples of \mathbf{x} have been used for the histogram. The standard Normal distribution is also plotted for comparison. Assuming RRC pulses with roll-off factor $\beta = 0.5$ and $\tau = \tau_0/2$ at TBP $\Omega = 50$.

identically distributed. Let $K_Y(t) = \ln \mathbb{E}\{e^{tY}\}$ be the cumulative generating function (CGF) of Y and $K'_Y(t)$ and $K''_Y(t)$ be 1st and 2nd derivatives of $K_Y(t)$, respectively. Then, due to Corollary 1 of [24], the logarithm of the CDF of Y may be approximated as

$$\ln P[Y \leq a] \approx \ln Q\left(\sqrt{\hat{t}^2 K''_Y(\hat{t})}\right) + K_Y(\hat{t}) - \hat{t} K'_Y(\hat{t}) + \frac{\hat{t}^2}{2} K''_Y(\hat{t}),$$

where $\hat{t} \leq 0$ satisfies $K'_Y(\hat{t}) = a$, when $a \leq \mathbb{E}[Y]$ and $\int_{-\infty}^{\infty} |x - K'_{X_n}(t)|^3 f_{X_n}(x) e^{x - K_{X_n}(t)} dx$ exist and are finite in a neighborhood of \hat{t} .

When applied to the meta-converse bound for FTN in Theorem 2, we get the following approximation for (19):

$$R \approx -\frac{1}{\Omega} \left[\ln Q\left(\sqrt{\hat{t}^2 K''(\hat{t})}\right) + K(\hat{t}) - \hat{t} K'(\hat{t}) + \frac{\hat{t}^2}{2} K''(\hat{t}) \right], \quad (33)$$

where $\hat{t} \leq 0$ satisfies $K'(\hat{t}) = N\lambda$ and

$$K(t) = \sum_{n=0}^{N-1} \left(\frac{(1+\sigma_n^2)t}{\sigma_n^2 - t} - \ln \left(1 - \frac{1}{\sigma_n^2} t \right) \right),$$

$$K'(t) = \sum_{n=0}^{N-1} \left(\frac{1}{\sigma_n^2 - t} \left(1 + \frac{1+\sigma_n^2}{1 - \frac{1}{\sigma_n^2} t} \right) \right), K''(t) = \sum_{n=0}^{N-1} \left(\frac{1}{(\sigma_n^2 - t)^2} \left(1 + \frac{2(1+\sigma_n^2)}{1 - \frac{1}{\sigma_n^2} t} \right) \right).$$

This result follows from the moment generating function (MGF) of $\mathcal{X}^2(1, \nu)$ being $M(t) = \frac{1}{1-t} \exp\left(\frac{t}{1-t} \nu\right)$ [35]. The approximation (33) is simple to compute due to its closed-form expression and \hat{t} can be found using any root-finding algorithms. Computing P_e (20), on the other hand, does not need such approximation since the range of P_e of interest are usually higher than 10^{-6} .

Similarly, applying the approximation to the RCU bound for FTN (29) in Theorem 4, we obtain

$$P_e \approx \mathbb{E}_{\tilde{\mathbf{x}}, \tilde{\mathbf{y}}} \left[\exp \left(\min \left\{ 0, \ln(2^{\Omega R} - 1) + \ln Q \left(\sqrt{\hat{\tau}_{\tilde{\mathbf{y}}}^2} K''(\hat{\tau}_{\tilde{\mathbf{y}}}) \right) \right. \right. \right. \\ \left. \left. \left. + K(\hat{\tau}_{\tilde{\mathbf{y}}}) - \hat{\tau}_{\tilde{\mathbf{y}}} K'(\hat{\tau}_{\tilde{\mathbf{y}}}) + \frac{\hat{\tau}_{\tilde{\mathbf{y}}}^2}{2} K''(\hat{\tau}_{\tilde{\mathbf{y}}}) \right\} \right) \right], \quad (34)$$

where $\hat{\tau}_{\tilde{\mathbf{y}}} \leq 0$ satisfies $K'(\hat{\tau}_{\tilde{\mathbf{y}}}) = \mu(\tilde{\mathbf{x}}, \tilde{\mathbf{y}})$ and

$$K(t) = \sum_{n=0}^{N-1} \left(\frac{|\tilde{y}_n|^2 t}{\sigma_n^2 - t} - \ln \left(1 - \frac{1}{\sigma_n^2} t \right) \right), \\ K'(t) = \sum_{n=0}^{N-1} \left(\frac{1}{\sigma_n^2 - t} \left(1 + \frac{|\tilde{y}_n|^2}{1 - \frac{1}{\sigma_n^2} t} \right) \right), K''(t) = \sum_{n=0}^{N-1} \left(\frac{1}{(\sigma_n^2 - t)^2} \left(1 + \frac{2|\tilde{y}_n|^2}{1 - \frac{1}{\sigma_n^2} t} \right) \right).$$

For $\Omega R \gg 0$, we can use $\ln(2^{\Omega R} - 1) \approx \Omega R \ln(2)$. We note that CGF $K(t)$ and its derivatives are all functions of $\tilde{\mathbf{y}}$, and $\hat{\tau}_{\tilde{\mathbf{y}}}$ must be found for each realization of $\tilde{\mathbf{y}}$. In our simulations, the expected value in (34) is numerically computed by taking a sample mean of at least 10^6 realizations of $\tilde{\mathbf{x}}$ and $\tilde{\mathbf{y}}$.

REFERENCES

- [1] J. B. Anderson, F. Rusek, and V. Öwall, "Faster-than-Nyquist signaling," *Proc. IEEE*, vol. 101, pp. 1817-1830, Aug. 2013.
- [2] J. Fan, S. Guo, X. Zhou, Y. Ren, G. Y. Li, and X. Chen, "Faster-than-Nyquist signaling: An overview," *IEEE Access*, vol. 5, pp. 1925-1940, 2017.
- [3] T. Ishihara, S. Sugiura, and L. Hanzo, "The evolution of faster-than-Nyquist signaling," *IEEE Access*, vol. 9, pp. 86535-86564, 2021.
- [4] F. Rusek and J. B. Anderson, "Constrained capacities for faster-than-Nyquist signaling," *IEEE Trans. Inform. Theory*, vol. 55, no. 2, pp. 764-775, Feb. 2009.
- [5] A. D. Liveris and C. N. Georghiades, "Exploiting faster-than-Nyquist signaling," *IEEE Trans. Commun.*, vol. 51, no. 9, pp. 1502-1511, Sep. 2003.
- [6] A. Prlja and J. B. Anderson, "Reduced-complexity receivers for strongly narrowband intersymbol interference introduced by faster-than-Nyquist signaling," *IEEE Trans. Commun.*, vol. 60, no. 9, pp. 2591-2601, Sep. 2012.
- [7] S. Sugiura and L. Hanzo, "Frequency-domain-equalization-aided iterative detection of faster-than-Nyquist signaling," *IEEE Trans. Veh. Tech.*, vol. 64, no. 5, pp. 2122-2128, May 2015.
- [8] Y. J. D. Kim, J. Bajcsy, and D. Vargas, "Faster-than-Nyquist broadcasting in Gaussian channels: Achievable rate regions and coding," *IEEE Trans. Commun.*, vol. 64, no. 3, pp. 1016-1030, Mar. 2016.
- [9] S. Li, J. Yuan, B. Bai, and N. Benvenuto, "Code-based channel shortening for faster-than-Nyquist signaling: Reduced-complexity detection and code design," *IEEE Trans. Commun.*, vol. 68, no. 7, pp. 3996-4011, Jul. 2020.
- [10] M. Shirvanimoghadam *et al.*, "Short block-length codes for ultra-reliable low latency communications," *IEEE Commun. Mag.*, vol. 57, no. 2, pp. 130-137, Feb. 2019.
- [11] ITU-R M.2083-0, IMT Vision – Framework and overall objectives of the future development of IMT for 2020 and beyond, Sep. 2015.
- [12] S. Das, N. Mohanty, and A. Singh, "Is the Nyquist rate enough?," in *Proc. Int. Conf. Digital Telecommun. (ICDT)*, Bucharest, Romania, pp. 27-32, Jun.-Jul. 2008.
- [13] M. Mohammadkarimi, R. Schober, and V. W. S. Wong, "Channel coding rate for finite blocklength faster-than-Nyquist signaling," *IEEE Commun. Letters*, vol. 25, no. 1, pp. 64-68, Jan. 2021.
- [14] Y. Polyanskiy, H. V. Poor, and S. Verdú, "Channel coding rate in the finite blocklength regime," *IEEE Trans. Inf. Theory*, vol. 56, no. 5, pp. 2307-2359, May 2010.
- [15] D. Slepian, "On bandwidth," *Proc. IEEE*, vol. 64, no. 3, pp. 292-300, Mar. 1976.
- [16] C. E. Shannon, "Communication in the presence of noise," *Proc. IRE*, vol. 37, no. 1, pp. 10-21, Jan. 1949.
- [17] Y. J. D. Kim and J. Bajcsy, "On spectrum broadening in pre-coded faster-than-Nyquist signaling," in *Proc. IEEE Veh. Tech. Conf. (VTC-Fall)*, 5 pages, Sep. 2010.
- [18] T. Ishihara and S. Sugiura, "Eigendecomposition-precoded faster-than-Nyquist signaling with optimal power allocation in frequency-selective fading channels," *IEEE Trans. Wireless Commun.*, vol. 21, no. 3, pp. 1681-1693, Mar. 2022.
- [19] Y. J. D. Kim, "Properties of faster-than-Nyquist channel matrices and folded-spectrum, and their properties," in *Proc. IEEE Wireless Commun. Netw. Conf. (WCNC)*, Doha, Qatar, pp. 1982-1988, Apr. 2016.
- [20] T. M. Cover, J. A. Thomas, *Elements of Information Theory*. New York: Wiley-Interscience, 1991.
- [21] T. Erseghe, "Coding in the finite-blocklength regime: Bounds based on Laplace integrals and their asymptotic applications," *IEEE Trans. Inform. Theory*, vol. 62, no. 12, pp. 6854-6883, Dec. 2016.
- [22] M. C. Gursoy, "Throughput analysis of buffer-constrained wireless systems in the finite blocklength regime," *EURASIP J. Wireless Commun. Netw.*, vol. 2013, no. 290, 13 pages, 2013.
- [23] J. Font-Segura, G. Vazquez-Vilar, A. Martinez, A. Guillén i Fàbregas, and A. Lancho, "Saddlepoint approximations of lower and upper bounds to the error probability in channel coding," in *Proc. 52nd Annual Conf. Inform. Sci. Syst. (CISS)*, Princeton, NJ, USA, pp. 1-6, Mar. 2018.
- [24] J. A. Maya, L. R. Vega, and C. G. Galarza, "A closed-form approximation for the CDF of the sum of independent random variables," *IEEE Signal Process. Lett.*, vol. 24, no. 1, pp. 121-125, Jan. 2017.
- [25] S. Verdú and T. S. Han, "A general formula for channel capacity," *IEEE Trans. Inf. Theory*, vol. 40, no. 4, pp. 1147-1157, Jul. 1994.
- [26] G. Durisi and A. Lancho. (2020). Lecture notes: Transmitting short packets over wireless channels – an information theoretic perspective. Available: <https://gdurisi.github.io/fbl-notes/index.html>.
- [27] J. Scarlett, V. Y. F. Tan, and G. Durisi, "The dispersion of nearest-neighbor decoding for additive non-Gaussian channels," *IEEE Trans. Inform. Theory*, vol. 63, no. 1, pp. 81-92, Jan. 2017.
- [28] Y. G. Yoo and J. H. Cho, "Asymptotic optimality of binary faster-than-Nyquist signaling," *IEEE Commun. Letters*, vol. 14, no. 9, pp. 788-790, Sep. 2010.
- [29] K. Masaki, T. Ishihara, and S. Sugiura, "Tradeoff between calculation precision and information rate in eigendecomposition-based faster-than-Nyquist signaling," *IEEE Access*, vol. 8, pp. 223461-223471, 2020.
- [30] E. Cerci, A. Dıcek, E. Cavus, E. Bedeer, and H. Yanikomeroglu, "Coded faster-than-Nyquist signaling for short packet communications," in *Proc. IEEE Annu. Int. Symp. Pers., Indoor Mobile Radio Commun. (PIMRC)*, Virtual, pp. 428-433, Sep. 2021.
- [31] A. A. Siddiqui, E. Bedeer, H. H. Nguyen, and R. Barton, "Spectrally-efficient modulation on conjugate-reciprocal zeros (SE-MOCZ) for non-coherent short packet communications," *IEEE Trans. Wireless Commun.* (Early Access).
- [32] I. Kanaras, A. Chorti, M. R. D. Rodrigues, and I. Darwazeh, "Spectrally efficient FDM signals: Bandwidth gain at the expense of receiver complexity," in *Proc. IEEE Int. Conf. Commun. (ICC)*, pp. 1-6, Jun. 2009.
- [33] Y. J. D. Kim and Y. Feng, "Capacity of multicarrier faster-than-Nyquist signaling," in *Proc. IEEE Int. Symp. Inf. Theory (ISIT)*, Los Angeles, CA, USA, pp. 2067-2072, Jun. 2020.
- [34] S. Wen, G. Liu, F. Xu, L. Zhang, C. Liu, and M. A. Imran, "Ergodic capacity of MIMO faster-than-Nyquist transmission over triply-selective Rayleigh fading channels," *IEEE Trans. Commun.*, vol. 70, no. 8, pp. 5046-5058, Aug. 2022.
- [35] G. L. Turin, "The characteristic function of Hermitian quadratic forms in complex normal variables," *Biometrika*, vol. 47, no. 1/2, pp. 199-201, Jun. 1960.